ELectronics EXpress

IEICE Electronics Express, Vol.16, No.7, 1–6

LETTER

A compact FSS with dual passbands and wide stopband

Zuxue Xia[1,2a)], Falin Liu[1], Xianfa Tang[3], Xin Cao[2], and Qiangming Cai[2]

Abstract A novel compact multi-band frequency selective surface (FSS) with dual passbands and wide upper stopband is presented. The proposed FSS was originally a double-layer structure. The grid-double square loops (G-DSLs) are located at the bottom to achieve the dual passband characteristics. In order to realize wide upper stopband, a modified square ring and a Jerusalem cross (M-SR-JC) element structure at top and bottom are used. Considering the higher power engineering applications, the final FSS uses a multi-layer structure. The FSS provides two pass-bands centered at 3.8 and 5.8 GHz with relative bandwidths of 18.4% and 13.5%, respectively. It also provides wide stopband characteristics from 10.8 GHz to 14.5 GHz. The simulation and measurement are in good agreement. The novel FSS with dual passbands and wide upper stopband is compact; easy to design and fabricate, and achieves relatively stable multi-band response under different polarization states and different incident angles. The proposed FSS can better meet the engineering requirements.

Keywords: dual passband, wide stopband, FSS, M-SR-JC element, compact, polarization stability

Classification: Microwave and millimeter-wave devices, circuits, and modules

1. Introduction

A frequency-selective surface (FSS) is essentially an electromagnetic spatial filter with a conventional planar two-dimensional periodic array structure. When the incident electromagnetic wave frequency is at the resonant frequency of the aperture type or patch type unit, the FSS will exhibit significant bandpass or bandstop filter characteristics [1, 2]. FSSs have widely been used in spatial filters, absorbers, antenna radomes, and electromagnetic compatibility in the microwave, millimeter-wave and taraherz ranges [3, 4, 5, 6].

In recent years, the FSS with simple shape and closely spaced multi-band resonance of miniaturized size and stable response becomes a research hotspot because of the increasing demands on multi-functionality of antennas and filters for both commercial and military applications [7, 8]. Dual [9, 10, 11, 12, 13, 14], triple [15, 16, 17] and wideband [18, 19] FSSs can be used for communication filtering, absorbing or electromagnetic interference (EMI) shielding. However, few can be applied to the passband with wide stopband [20, 21]. There is currently no mention or report in published literatures that FSS can withstand higher power in practical applications.

Several technologies can be applied to design the multi-band FSS: (1) combination of multi-resonant units [22, 23, 24]; (2) utilization of two or more layer structures [25, 26, 27]; (3) fractal element [28, 29] and (4) three-dimensional topology element [30, 31].

However, there are some challenges to be considered for multi-band FSSs. A single layer has not good angular stability and polarization stability; a fractal structure is hard to design, although the structure has self-similarity feature that results in a multiband property; 3D structures can provide better performance, but vias are generally required, which are difficult to fabricate; complicated planar structures can have a miniaturized structure, but are difficult to design, while conventional structures have larger size unit cells, which will yield larger size FSSs.

In this letter, a multi-layer compact FSS unit with dual passbands and wide upper stopband is proposed. The FSS with G-DSLs at bottom provides two pass-bands centered at 3.8 and 5.8 GHz with relative bandwidths of 18.4% and 13.5%, respectively. The FSS with M-SR-JC element at bottom and top also provides wide stopband characteristics from 10.8 GHz to 14.5 GHz. The novel FSS has advantages of compact size, ease of design and handling, with better stable multi-band response at different polarization states and different angles of incidence. It can better realize the transmission characteristics in C and S band, and complete the reflection characteristics in Ku band.

2. Unit cell geometry

An FSS adopts a single layer or a double-layer board which is simple in structure and easy to fabricate. The cell structure of the proposed double-layer FSS consists of a two-part structural unit, as shown in Fig. 1. The first part is a combination of an enhanced M-SR-JC element on both sides of the top and bottom, which provides a wide stopband characteristics and high out-of-band rejection at the transition frequencies; the other part is a G-DSLs structure at the bottom side to provide dual passbands.

In order to meet the demand for higher power capacity, the FSS requires a support structure with better wave transmission performance and structural strength. A multi-layer structure is used here, as shown in Fig. 2:

As can be seen from Fig. 2, the structure is divided into 5 layers. The yellow part is the FSS copper surface on the top and bottom surfaces of layer 2. The materials and the parameters of the five layers are shown in Table I:

[1]Dept. of Electronic Engineering and Information Science, USTC, Anhui, Hefei 230027, China
[2]Sch. of Information Engineering, SWUST, Sichuan, Mianyang 621010, China
[3]Sch. of National Defense Science and Technology, SWUST, Sichuan, Mianyang 621010, China
a) xiazuxue@mail.ustc.edu.cn

DOI: 10.1587/elex.16.20190067
Received February 1, 2019
Accepted February 19, 2019
Publicized March 1, 2019
Copyedited April 10, 2019

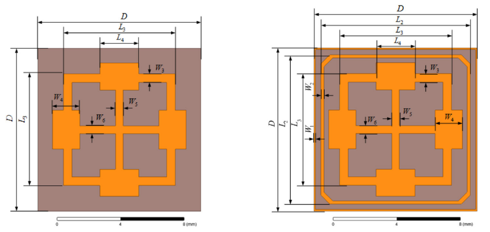

(a) (b)

Fig. 1. Proposed FSS Unit Cell (a) Top view. (b) Bottom view.

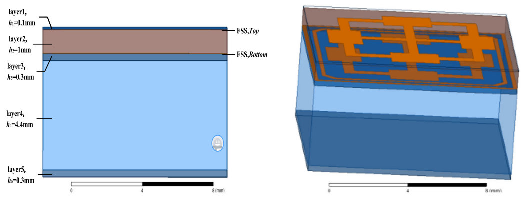

(a) (b)

Fig. 2. Proposed FSS (a) side view (b) 3D view

Table I. Materials and relative permittivity of the five layers

layer1	layer2	layer3	layer4	layer5
Protective film	F4B-2	Upper support	Honeycomb sandwich	Lower support
ε_{r1}	ε_{r2}	ε_{r3}	ε_{r4}	ε_{r5}
2.5	2.65	2.5	1.1	2.5

Different from structures in literature [27] which have different patterns on different layers, for the multilayer structure here, the metal FSS structure only exists on the top and bottom surfaces of layer 2. The multi-layer FSS also have dual passbands and wide upper stopband characteristics. Besides, the FSS is compact, easy to design and fabricate.

3. Gridded square loops unit and evolution of the wide stopband unit cell

In order to achieve the proposed FSS with dual passbands and upper wide stopband characteristics, the FSS cell design includes two partial structural designs.

The shape of the unit cell determines the frequency response characteristics, and the size of the unit cell determines the operating frequency of the FSS. For a square ring or a circular ring, the circumference is proportional to the wavelength of resonance. A square ring is more compact than a circular ring.

In order to achieve the dual passbands characteristics, the reference [9] uses a single-layer metal structure, which is etched with dual-concentric square slots only on top side, as shown in Fig. 3.

The design contains a F4B-2 substrate thickness of 1 mm with dielectric constant of 2.65 and the loss tangent of 0.001. Here, the structural parameters have been modified, the aperture gap width of W_{g1} is constant, and only the W_{g2} parameter is changed. Using the full-wave EM simulator HFSS, the simulated results of the FSS with different width of W_{g2} are shown in Fig. 4.

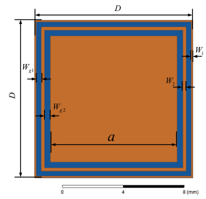

Fig. 3. The Structure of the dual-band bandpass FSS with the dimensions $D = 10.5$ mm, $a = 8.4$ mm, $Wg_1 = 0.4$ mm, $W1 = 0.1$ mm

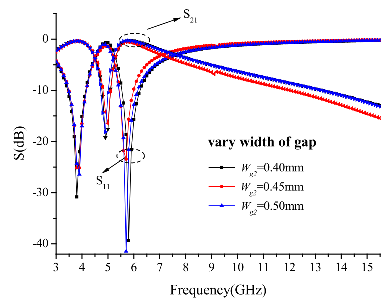

Fig. 4. Simulated scattering parameters of the FSS with different aperture gap widths for normal incidence

It can be seen from Fig. 4 that the first resonance frequency is unchanged, while the second resonance frequency changes with W_{g2}. When W_{g2} is equal to 0.4 mm, there is a better dual passbands' characteristics, the dual passbands are at 3.8 and 5.8 GHz with insertion loss of 0.32 dB and 0.22 dB. We also find that the rejection is less than 10 dB around the upper transition frequencies of the second passband up to 12.4 GHz, and this does not meet the wide stopband characteristics from 10.8 GHz to 14.5 GHz.

Compared with single-side etching, the double-side etching can have better frequency response characteristics. In order to achieve wide stopband characteristics in Ku band and solve the problem of low rejection at the transition frequencies, a double-side enhanced M-SR-JC element is adopted here. Evolution process of the proposed unit is illustrated in Fig. 5.

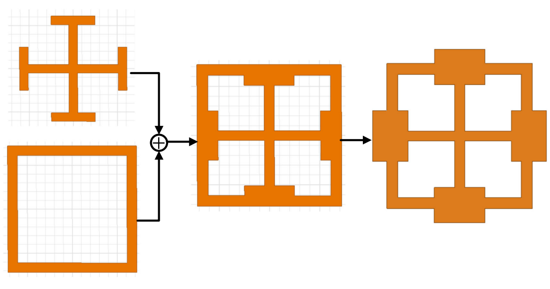

(a) (b) (c)

Fig. 5. Evolution process of the unit cell of the wide stopband FSS

With two or more patch-type resonant structures with similar resonant frequencies, wide stopband characteristics can also be achieved. The most common wide stopband structure is the Jerusalem cross patch structure [18, 19], while the square ring patch structure is a narrow stopband structure. So in Fig. 5, the two different structures of (a) are combined into one unit (b), making the structural unit more compact. In order to obtain better frequency stability, the pattern (c) is obtained to form a compact wide stopband FSS unit, and the unit is symmetrical in nature resulting in good incidence polarization stability [9, 10].

For normal incident wave, the simulation results of the wide stopband FSS at different evolution stages are shown in Fig. 6. The M-SR-JC element has better wide stopband characteristics than the other two structures.

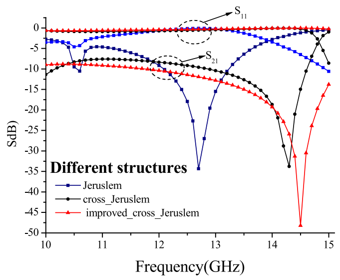

Fig. 6. Comparison of simulated results of the wide stopband FSSs with different structures in Ku band with the dimensions $D = 10.5\,\text{mm}$, $L_3 = 7.2\,\text{mm}$, $W_3 = 0.2\,\text{mm}$, $L_4 = 2.5\,\text{mm}$, $W_4 = 1.75\,\text{mm}$, $W_5 = 0.5\,\text{mm}$, $W_6 = 0.5\,\text{mm}$ (Refer to Fig. 1 for dimension captions)

Considering the good wide stopband structure, the central metal patch structure of Fig. 3 is replaced, thus forming a metal patch G-DSLs structure at the bottom, combined with the M-SR-JC element at both the top and bottom, ultimately forming the structure of Fig. 1.

4. Simulation and discussion

In addition, the inner square ring is chamfered to improve the out-of-band rejection of the transition regions between the C-band and Ku-band. The main parameters of the optimized unit size are shown in Table II:

Table II. The proposed FFS physical layout size (UNIT: mm)

D	L_2	L_3	L_4	W_5
10.5	9.6	7.2	2.5	0.5
W_1	W_2	W_3	W_4	W_6
0.1	0.2	0.45	1.75	0.5

The simulated results of the proposed FSS for both TE and TM polarizations under various incident angles are shown in Fig. 7(a) and (b), respectively:

Here, the angle of incidence of 0° to 30° is considered, and the step size is 10°. As can be seen from Fig. 7, the FSS model has good angular stability for both TE and TM polarizations. For TE and TM modes under normal incidence, the insertion loss in the low band is less than 1 dB; there is a transmission zero that exceeds −20 dB in the second passband and stopband transition regions. The transmission coefficient in Ku band is almost less than 10 dB, and the reflection coefficient is less than 1 dB from 10.8 GHz to 14.5 GHz.

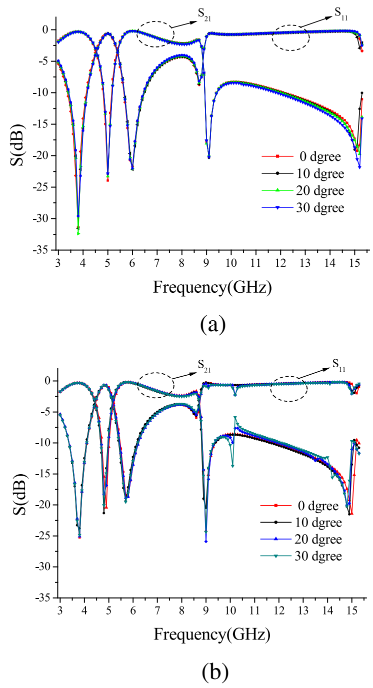

Fig. 7. Simulated scattering parameters of the proposed FSS for different incident angles under (a) TE and (b) TM polarizations

To illustrate the physical mechanism forming dual passbands and a wide stopband, the electric field distribution of the FSS surface when operating at the low and high frequency bands under normal incidence is shown in Fig. 8 and 9, respectively.

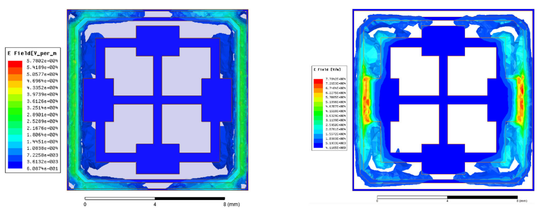

(a) (b)

Fig. 8. Electric field distribution of the FSS at low frequency bands. (a) $f = 3.8\,\text{GHz}$ (b) $f = 5.8\,\text{GHz}$.

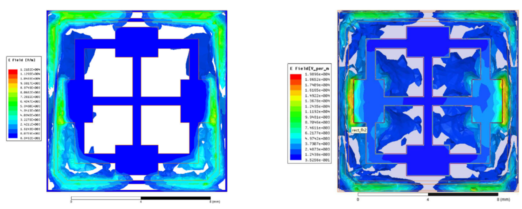

(a) (b)

Fig. 9. Field distribution of the FSS at high frequency bands. (a) $f = 11.2\,\text{GHz}$ (b) $f = 14.2\,\text{GHz}$.

The electric field distribution is the same under normal incident angle for TE and TM polarizations. As can be observed from Fig. 8 and 9, the electric field focused on outer slot and the gap between inner square ring and M-SR-JC element, implying that the first resonance frequency is decided by outer slot, and the second resonance frequency is decided by the gap between inner square ring and M-SR-JC element, while the wide stopband is decided by the M-SR-JC element.

5. Experimental setup and measurement results verification

The final fabricated compact FSS is shown in Fig. 10. The FSS prototype has a total of more than 600 unit structures with a diameter of Φ300 mm.

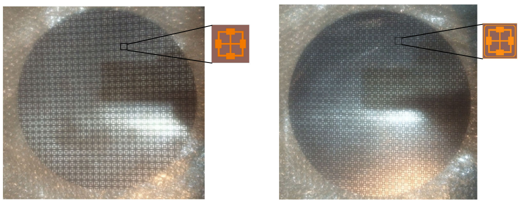

(a) (b)

Fig. 10. Photograph of the fabricated FSS (a) top view (b) back view

The FSS measurement environment is shown in Fig. 11. It is generally measured in an anechoic room using a free space transmission method. It is mainly composed of the FSS screen, a pair of transmitting and receiving antennas, and a vector network analyzer. The distance between the transceiver horn antennas and the FSS under test needs to meet the far field radiation condition. To reduce the effect of the edge effect on the test, two absorption screens are placed next to the FSS prototype.

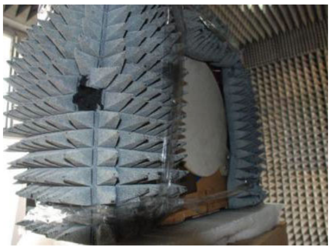

Fig. 11. FSS measurement environment.

So a complete test setup is shown in Fig. 12. The data are measured by a vector network analyzer (Agilent PNA-X).

The measured and simulated results under normal incidence are shown in Fig. 13.

As can be observed from Fig. 13, the measured results agree well with the simulated ones. The measured dual passbands are at 3.8 and 5.8 GHz with insertion loss of 0.13 dB and 0.24 dB and the fractional frequency bandwidths of about 18.4% and 13.5%, respectively. The reflection coefficient of Ku band is less than 1 dB from 10.8 to 14.5 GHz. The measured transmission coefficient occurs offset at high band; the reason is mainly attributed to fabrication errors and measurement errors.

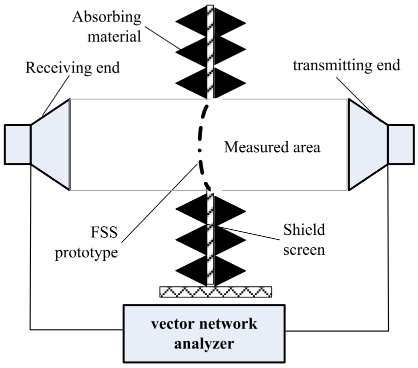

Fig. 12. Illustrations of the FSS test setup.

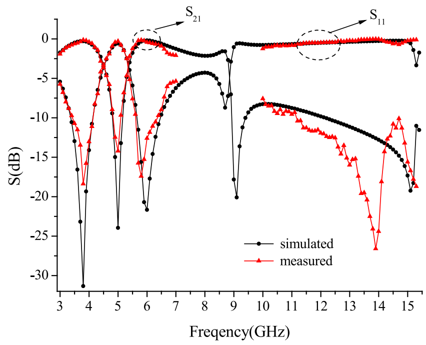

Fig. 13. The measured and simulated results of the proposed FSS.

Due to the limitations of the conditions, test at transition frequency regions are not available. However, from the simulation and test results, it is clear that the proposed FSS has dual passbands and wide stopband characteristics, which can meet the engineering requirements.

The comparisons of the proposed FSS with other reported ones are given in Table III.

Table III. Comparisons of the proposed FSS with previously designed structures

Ref.	Unit cell (mm^2)	NO. of bands	f_2/f_1	Comparison points of Operating frequency bands
9	24.4 × 24.4	2	1.53	Dual passbands in L and S band
10	10.4 × 10.4	2	1.39	Dual stopbands in S band
11	8.4 × 8.4	2	1.29	Dual stopbands in S band
18	12.0 × 12.0	1	-	Wide stopband in X and Ka band
20	6.0 × 4.5	1	-	One passband in S band with wideband spurious rejection
This Work	10.5 × 10.5	3	1.53	Dual passband in S and C band, and wide stopband in Ku band

As can be seen from Table III, only the proposed FSS has dual passbands and wide stopband characteristics, with a larger dual passbands frequency ratio and a smaller structural size. Compared with literature [9], when ensuring the excellent dual-passband characteristics, the wide stopband characteristics are added without increasing the relative structure size. The structures of literatures [10] and [11] are complex and difficult to design. Compared with the literature of [18], our structures increase the dual passbands characteristics. Although literature [20] has superior performance and small structure, there are 3D structures with metallic rods and plates, making it difficult to fabricate. In nature the structure of this paper is multi-layered, but the metal structure only exists in the top and bottom sides of one layer, making the design and fabrication are relatively easy.

Generally speaking, the proposed FSS structural unit has a smaller size and a larger dual passband frequency ratio, and wide upper stopband characteristics. Besides, the proposed FSS is easy to design and fabricate.

6. Conclusion

In this letter, a multi-layer FSS with dual passbands and wide stopband has been presented. The higher to lower center frequency ratio of the design turns out to be 1.53 with a unit cell of size $0.2\lambda \times 0.2\lambda$, where λ is the wave-length of the guided wave corresponding to the center frequency of the first pass band. Furthermore, the structure has been fabricated and measured. The simulation and measurement are in good agreement. Considering the need for higher power capacity, the novel multi-layer compact FSS has still a simple metal structure, only on both sides of the main dielectric layer, thus avoiding the problems of reported structures with via holes or different shapes of metal in different layers, so it is easy to design and fabricate. It also has a relatively stable multi-band response at different polarization states with different incident angles. The proposed FSS can better meet the practical engineering requirements.

Acknowledgments

This work is supported by National Science Foundation of China (No. 61801406), and Longshan Talent Fund of Southwest University of Science and Technology (SWUST) (No. 18lzx677).

References

[1] B. A. Munk: *Frequency Selective Surfaces: Theory and Design* (Wiley, NewYork, 2000).
[2] Y.-K. Cho, *et al.*: "Experimental verification of electromagnetic scattering via two-dimensional periodic array of small resonant apertures," IEICE Electron. Express **14** (2017) 20170796 (DOI: 10.1587/elex.14.20170796).
[3] R. Anwar, *et al.*: "Frequency selective surfaces: A review," Applied Sciences **8** (2018) 1689 (DOI: 10.3390/app8091689).
[4] P. Mei, *et al.*: "A low radar cross section and low profile antenna co-designed with absorbent frequency selective radome," IEEE Trans. Antennas Propag. **66** (2018) 409 (DOI: 10.1109/TAP.2017.2767645).
[5] W. Mohyuddin, *et al.*: "A practical double-sided frequency selective surface for millimeter-wave applications," Rev. Sci. Instrum. **89** (2018) 024703 (DOI: 10.1063/1.5023406).
[6] H. Lu, *et al.*: "Measurement of LC dielectric constant at lower terahertz region based on metamaterial absorber," IEICE Electron. Express **14** (2017) 20170469 (DOI: 10.1587/elex.14.20170469).
[7] P. P. Sarkar: "Frequency selective surfaces: Development and prospect," Proceedings of the Third International Conf. on C3IT (2015) 7060107 (DOI: 10.1109/C3IT.2015.7060107).
[8] G. Naym, *et al.*: "Multi-band feed assembly for linear and circular polarization," U.S. Patent 8994473 (2015).
[9] Y. Yang, *et al.*: "Dual-band frequency selective surface with miniaturized element in low frequencies," PIER Lett. **33** (2012) 167 (DOI: 10.2528/PIERL12070319).
[10] R. Sivasamy and M. Kanagasabai: "A novel dual-band angular independent FSS with closely spaced frequency response," IEEE Microw. Wireless Compon. Lett. **25** (2015) 298 (DOI: 10.1109/LMWC.2015.2410591).
[11] S. Ghosh and K. V. Srivastava: "An angularly stable dual-band FSS with closely spaced resonances using miniaturized unit cell," IEEE Microw. Wireless Compon. Lett. **27** (2017) 218 (DOI: 10.1109/LMWC.2017.2661683).
[12] F. C. G. da Silva Segundo and A. L. P. S. Campos: "A compact frequency selective surface with dual band response for WLAN applications," Microw. Opt. Technol. Lett. **57** (2015) 265 (DOI: 10.1002/mop.28830).
[13] X.-J. Sheng, *et al.*: "A miniaturized dual-band FSS with controllable frequency resonances," IEEE Microw. Wireless Compon. Lett. **27** (2017) 915 (DOI: 10.1109/LMWC.2017.2746680).
[14] S. Can, *et al.*: "A dual-band polarization independent FSS having a transparent substrate for ISM and Wi-Fi shielding," Microw. Opt. Technol. Lett. **59** (2017) 2249 (DOI: 10.1002/mop.30715).
[15] M. Yan, *et al.*: "A tri-band, highly selective, band-pass FSS using cascaded multilayer loop arrays," IEEE Trans. Antennas Propag. **64** (2016) 2046 (DOI: 10.1109/TAP.2016.2536175).
[16] M. Bashiri, *et al.*: "WiMAX, WLAN, and X band filtering mechanism: Simple-structured triple-band frequency selective surface," IEEE Antennas Wireless Propag. Lett. **16** (2017) 3245 (DOI: 10.1109/LAWP.2017.2771265).
[17] P. Mei, *et al.*: "A triple-band absorber with wide absorption bandwidths using impedance matching theory," online published by IEEE Antennas Wireless Propag. Lett. (2019) (DOI: 10.1109/LAWP.2019.2895971).
[18] I. S. Syed, *et al.*: "A single layer frequency-selective surface for ultra-wideband electromagnetic shielding," IEEE Trans. Electromagn. Compat. **56** (2014) 1404 (DOI: 10.1109/TEMC.2014.2316288).
[19] A. Kesavan, *et al.*: "A novel wideband frequency selective surface for millimeter-wave applications," IEEE Antennas Wireless Propag. Lett. **15** (2016) 1711 (DOI: 10.1109/LAWP.2016.2528221).
[20] B. Li and Z. Shen: "Bandpass frequency selective structure with wideband spurious rejection," IEEE Antennas Wireless Propag. Lett. **13** (2014) 145 (DOI: 10.1109/LAWP.2014.2299278).
[21] Q. Li, *et al.*: "A novel miniaturized-element frequency selective surface with a second-order bandpass response," IEICE Electron. Express **15** (2018) 20171257 (DOI: 10.1587/elex.15.20171257).
[22] W. Li, *et al.*: "A FSS of hybrid combined elements for dual-band operations," IEICE Electron. Express **14** (2017) 20171008 (DOI: 10.1587/elex.14.20171008).
[23] P.-S. Wei, *et al.*: "Design and analysis of an ultraminiaturized frequency selective surface with two arbitrary stopbands," online published by IEEE Trans. Electromagn. Compat. (2018) 1 (DOI: 10.1109/temc.2018.2864546).
[24] B. Rahmati and H. R. Hassani: "Multiband metallic frequency selective surface with wide range of band ratio," IEEE Trans. Antennas Propag. **63** (2015) 3747 (DOI: 10.1109/TAP.2015.2438340).
[25] Q. Wang, *et al.*: "A dual-layer radar absorbing material with fully embedded square-holes frequency selective surface," IEEE Antennas Wireless Propag. Lett. **16** (2017) 3200 (DOI: 10.1109/LAWP.2017.2768441).
[26] M. N. Hussein, *et al.*: "A miniaturized low-profile multilayer frequency-selective surface insensitive to surrounding dielectric materials," IEEE Trans. Microw. Theory Techn. **65** (2017) 4851 (DOI: 10.1109/TMTT.2017.2709317).
[27] K. Tao, *et al.*: "Multi-layer tri-band frequency selective surface using stepped- and uniform-impedance resonators," Electronics

Lett. **53** (2017) 324 (DOI: 10.1049/el.2016.4469).

[28] X.-J. Sheng, *et al.*: "A dual-band fractal FSS with SZ curve elements," IEICE Electron. Express **14** (2017) 20170518 (DOI: 10.1587/elex.14.20170518).

[29] J. Romeu and Y. Rahmat-Samii: "Fractal FSS: A novel dual-band frequency selective surface," IEEE Trans. Antennas Propag. **48** (2000) 1097 (DOI: 10.1109/8.876329).

[30] A. K. Rashid, *et al.*: "An overview of three-dimensional frequency-selective structures," IEEE Antennas Propag. Mag. **56** (2014) 43 (DOI: 10.1109/MAP.2014.6867682).

[31] A. A. Omar and Z. Shen: "Multiband high-order bandstop 3-D frequency-selective structures," IEEE Trans. Antennas Propag. **64** (2016) 2217 (DOI: 10.1109/TAP.2016.2546967).